

## Two-Dimensional Monte Carlo Simulation of Boron Implantation in Crystalline Silicon

Gerhard Hobler, Hans Pötzl\*

*Institut für Allgemeine Elektrotechnik und Elektronik, TU Vienna, A-1040 Vienna, Austria*

\* also: *Ludwig-Boltzmann-Institut für Festkörperphysik, A-1060 Vienna, Austria*

Li Gong, Heiner Ryssel\*

*Fraunhofer-Arbeitsgruppe für Integrierte Schaltungen, D-8520 Erlangen, Germany*

\* also: *Lehrstuhl für Elektronische Bauelemente, D-8520 Erlangen, Germany*

### Abstract

We review the physical and numerical models used for Monte Carlo simulations of ion implantation in crystalline targets. Results of two-dimensional simulations of boron implantation in crystalline silicon are presented. Good agreement is found with equiconcentration lines near a mask edge obtained experimentally with a delineation technique. Differences between the dopant distributions in crystalline and amorphous silicon are discussed.

Two-dimensional Monte Carlo simulations of ion implantation in crystalline silicon have been of limited use because of prohibitive computation times and lack of agreement with experiments even in 1-D. Therefore, only a few reports on 2-D simulations can be found in the literature [1], [2], [3]. The first problem, although still an obstacle, has been relieved by the increase in computer power. The latter has given rise to research activities over the years. In particular, electronic stopping has received much attention [4], [5]. Recently, a model has been introduced [6] which is able to predict the range of boron channeled along various crystallographic axes. In view of 2-D simulations it is important that not only ions channeled in the  $\langle 100 \rangle$  direction are treated properly but also in other major directions like  $\langle 110 \rangle$ . As most channeling in  $\langle 100 \rangle$  wafers usually occurs in the  $\langle 100 \rangle$  direction, ions channeled in other directions might not show up in the 1-D profile, but may penetrate in the 2-D case into regions where otherwise no ions would be found. Using this electronic stopping power model, because of the physical nature of Monte Carlo simulations good results in 2-D can be expected. As will be shown, good agreement with 2-D experiments is indeed found. This, in turn, confirms the models used in the simulation. Before the 2-D simulations will be discussed, we review the basic physical and numerical models.

## 1 Physical Models

*Binary collision approximation:* The assumption of independent two-body interactions with the target atoms is inherent in all Monte Carlo simulations. Even when "simultaneous collisions" with two or more target atoms are taken into account [7], such an event is treated by evaluating the collisions with each of the atoms separately. After the direction and the energy of the recoils is determined, the new direction of the ion is calculated by applying momentum conservation to

ion and recoiled target atoms. The ion energy is obtained by scaling the energy of the ion and the recoils such that energy conservation is fulfilled. It is clear that such an approach is only approximate, as after energy conservation has been applied momentum conservation is violated. Errors will be negligible if at all times (a) one interaction dominates, or (b) all collisions taking place at the same time would only slightly affect the ion path when treated as binary collisions. (b) is true because at such low interactions the ion energy does not change significantly during the collision and the recoil momentum can be calculated by assuming straight path and constant energy of the ion. Once the momentum of the recoils is known, the small deflection angle of the ion is uniquely determined by momentum conservation. Under channeling conditions, even if (a) does not hold, (b) will usually hold as scattering angles of channeled ions are small. It should be mentioned that these considerations are in contrast to claims in the literature [3], [8].

In order to verify the above considerations, we have simulated the trajectories of a boron ion passing by two silicon atoms, using the binary collision approximation and solving Newton's equation with a time step method, respectively. Various impact parameters with respect to the two silicon atoms have been used. We found that errors of the scattering angle are well below  $0.1^\circ$  at 1 keV and decrease rapidly at higher energies. This also confirms earlier results obtained by using the MARLOWE code [9] with and without simultaneous collisions [10]. Below 1 keV we did not observe a striking advantage of the simultaneous collision model over subsequent collisions. We use the simultaneous collision model nevertheless for numerical reasons (see below) and because it requires no extra CPU time.

*Interatomic potential:* The most-widely used potentials are the Moliere and the universal ZBL potential [11]. It has been reported that no significant difference between the two is found for boron implantations in crystalline silicon [10]. Recently, it was claimed that the analytical approximations contained in the *universal* ZBL potential introduce significant errors into channeling simulations as compared with the *specific* B-Si ZBL potential [12]. It was argued that universal and specific potential deviate strongly at large atomic separations. However, this can hardly be understood, as the deviations become significant only beyond 2.5 Å. In comparison, the radius of the most open channel, the  $\langle 110 \rangle$  channel, is 2.0 Å. Therefore we consider the universal ZBL potential as sufficient.

*Electronic stopping power:* It has been known for a long time [13] that channeled ions experience reduced electronic stopping as compared with ions moving in a random direction. Models have been proposed [14], [15], [9], but they have not found experimental verification. Recently, a local-electron-density dependent model has been proposed [5]. Good agreement with experimental implantation profiles in  $\langle 100 \rangle$  wafers has been demonstrated. Also recently, another model has been introduced [6] which is not only capable of describing  $\langle 100 \rangle$  channeling properly, but also channeling in other directions such as  $\langle 110 \rangle$ . It is similar to that contained in MARLOWE. It reads

$$\Delta E_e^{nl} = N \cdot S_e \cdot \Delta R \cdot \left[ x^{nl} + x^{loc} \cdot \left( 1 + \frac{p_{max}}{a} \right) \cdot \exp \left\{ -\frac{p_{max}}{a} \right\} \right] \quad (1)$$

$$\Delta E_e^{loc} = x^{loc} \cdot \frac{S_e}{2\pi a^2} \cdot \exp \left\{ -\frac{p}{a} \right\} \quad (2)$$

$$S_e = k \cdot \sqrt{E}, \quad x^{nl} + x^{loc} = 1, \quad a = f \cdot \frac{a_{12}}{0.3} \quad (3)$$

(1) is taken into account during the free flight paths (length  $\Delta R$ ), and (2) at each collision (impact parameter  $p$ ).  $p_{max}$  is the maximum impact parameter allowed in a collision and should be large enough to ensure that the second term in (1) is negligible. We use  $p_{max} = 2.35$  Å.  $a_{12}$  denotes the screening length of the interatomic potential.

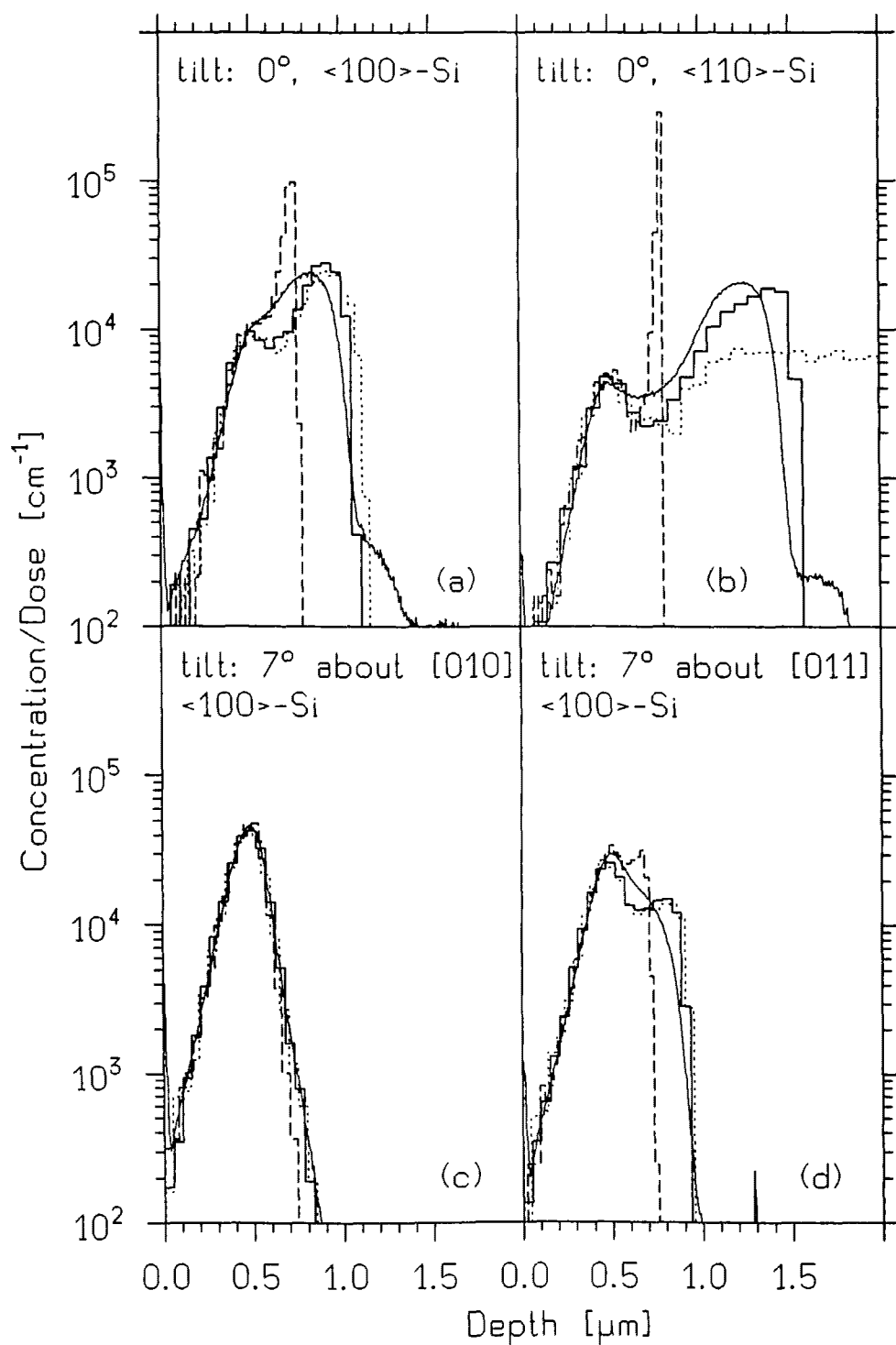


Figure 1: Boron in  $\langle 100 \rangle$  and  $\langle 110 \rangle$  silicon at 150 keV,  $10^{13} \text{ cm}^{-2}$ . Full line: experiment. Histograms: simulation using the Lindhard model (dashed), the Oen-Robinson model (dotted), and the new model (full).

In amorphous targets, (1)–(3) reduce to the Lindhard model [16] independent of the parameters, if Lindhard's value  $k_L$  is used for  $k$ . The model contains the Lindhard model ( $x^{loc} = 0$ ) and the Oen-Robinson model ( $x^{loc} = 1, f = 1$ ) as special cases. The parameters have been determined from carefully selected channeling experiments at 17 keV and 150 keV. At both energies  $k = 1.5k_L$ ,  $x^{nl} = 0.4$ , and  $f = 0.8$  yield good results. Figure 1 shows the comparison with experiments at 150 keV [6].

*Lattice vibrations:* Thermal vibrations of lattice atoms are essential for obtaining reasonable channeling results. Lattice vibrations are the dominating dechanneling mechanism unless the target contains considerable damage. As usual, we take the amplitude of the atomic displacements according to the Debye theory [17], the displacements are assumed to be uncorrelated and to be Gaussian distributed. The Debye theory is in good agreement with X-ray diffraction experiments. Moreover, it has been shown that correlations between the thermal vibrations of neighbouring atoms are very small [18].

## 2 Numerical Models

*Starting point:* In the simulation of ion implantation in crystalline targets the only two random processes are the selection of the starting points of the trajectories and the thermal vibrations of the target atoms. Therefore a statistically correct distribution of the entrance point into the crystal is essential. We assume that all ions shall enter in the same small area. It is clear that not all ions may start at exactly the same point. If, e. g., this point is close to a lattice site, all ions will undergo a heavy first collision. This obviously is not statistically correct. If the surface is a (100) plane, one may simply equidistribute the starting point within a square with an edge length equal to the lattice constant. For general wafer orientations we use the following algorithm: We produce equidistributed points inside the cubic unit cell and project these points to the surface in order to obtain the starting points. This can be justified as follows: The projection of all lattice sites to the surface is what the ion sees when it approaches the target. As the crystal is periodic with the three unit cell edges, the projection will be periodic with the projections of the three unit cell edges. If the surface is not a (100) plane, for each point inside the projection of the unit cell there will be one or more equivalent points inside the projection of the unit cell. The probability to hit one of the points is proportional to the length inside the unit cell of the line perpendicular to the surface going through the point. It may be shown that the sum of the lengths corresponding to equivalent points is a constant for a given surface orientation. Therefore, if we identify equivalent points, each point on the surface will be hit with the same probability.

The straightforward method to equidistribute  $N$  points inside an area is to simply place each point randomly. This will produce fluctuations corresponding to the number  $N$ . In our case, each simulated ion represents many real ions. Therefore the fluctuations in the simulation will be much larger than those in reality. To reduce the fluctuations, one may think of producing equidistant points inside the area. This is possible if going from one point to the neighbour point produces only small changes in the resulting trajectory. As this is not easy to judge, it should be handled with care. A third model which is used in our code combines the advantages of the two methods: We divide the area into  $N$  equally sized subareas and put only one point into each of the subareas. Within each subarea, the exact position is randomly chosen. In this way any point of the area is selected with the same probability while the global equidistribution is better than random. Notice that in the method for the selection of the starting point the "area" is the 3-D unit cell. The principle, however, is general and can be used in any dimension.

*Selection of collision partners:* The selection of the target atom(s) from the lattice sites to take part in the next collision is the main characteristic of the Monte Carlo simulation of ion implantation in *crystalline* targets. The conventional method is to produce a small crystal starting with a reference lattice point such that all lattice sites are within a certain radius. During the simulation of a trajectory, the reference point is shifted to the lattice site of the last collision partner and the shifted crystal is searched for the next collision partner. We tried another method in order to save computation time. The diamond lattice may be divided into cubes with an edge length of a quarter unit cell edge. Considering symmetry operations, there are only four basic types of these small cubes. Using these cubes, a much smaller neighbour list must be searched every time. However, the determination of the correct subcube and the application of the symmetry operations is expensive. Consequently, this method was not as successful as we had hoped.

Numerical errors or the change in direction by collisions may lead to skipping of scattering events or multiple scattering from the same lattice site. For instance, a target atom which has been ahead of the ion before a collision with another atom may be behind the ion after that collision. Or a heavy collision may change the direction of motion such that a target atom which has already been hit is hit again. In order to avoid these problems, several methods are possible: One may retain lattice sites of old collision partners and exclude them from further collisions unless the ion has significantly changed its direction. One may not only search ahead of the ion but also a small distance behind it; or alternatively (as we do) treat collisions which are almost the same distance ahead of the ion simultaneously (see Section 1). In order to avoid such troubles, we also neglect the "time integral" and assume that the deflection takes place in the foot of the impact parameter on the original direction of motion. Investigations, carried out by solving Newton's equation, indicate that the neglect of the time integral is justified as long as the binary collision approximation holds. Also, we allow the atoms to vibrate only perpendicular to the direction of ion motion. This is not expected to have any influence on the ion trajectory but avoids skipping of collisions.

It should be mentioned that these problems should not only be avoided in view of scattering but also in view of impact-parameter-dependent electronic stopping. Take, as an example, an ion moving in a  $\langle 110 \rangle$  channel parallel to the axis. It collides at the same point with four target atoms. If these collisions are treated subsequently and only atoms ahead of the ion are considered, one or two of them are likely to be skipped. This might not influence the direction of motion significantly as the interaction is weak. But there are also contributions to the electronic stopping being lost, i. e. the electronic stopping in the channel appears smaller and less determined than in the actual model.

*Interfaces:* For channeling simulations it is important to include a native oxide of 1–2 nm. Also, often the effect of an oxide or any other layer on the doping profile is of interest. The trajectories in the oxide may easily be simulated using standard methods [19]. However, care must be taken at the interface. A problem can occur when the ion moves across the interface with a grazing angle. If an atomic plane of the crystal is located immediately (less than 1 Å) below the interface and the ion is not able to collide with them as long as it is in the oxide, it will likely undergo a close collision when it enters the crystal. Therefore one either has to take care that the ion is able to collide with atoms in the neighbour region when it is near to the interface, or one has to introduce a small spacing between the layers.

*Evaluation of scattering angles:* Scattering angle and energy loss are calculated as usual from the center-of-mass scattering angle  $\theta$ .  $\theta$  as a function of reduced energy and impact parameter can be obtained from tabulated values. As has been reported earlier [20], using  $\cot \frac{\theta}{2}$

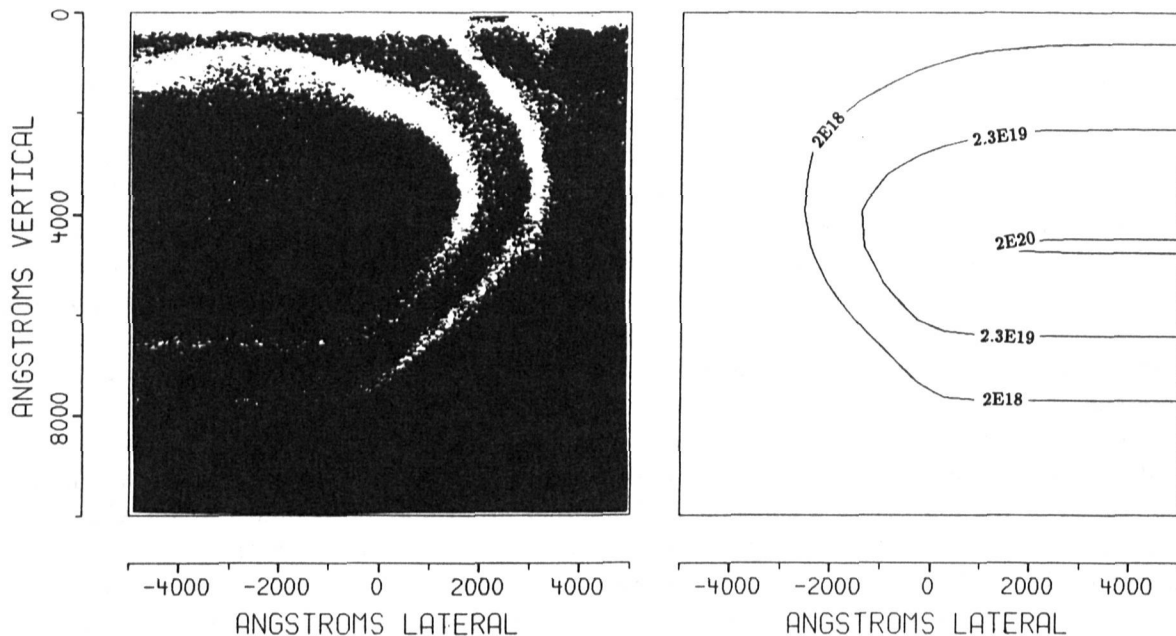


Figure 2: SEM micrograph of the boron implantation ( $140 \text{ keV}$ ,  $5 \cdot 10^{15} \text{ cm}^{-2}$ ) and the corresponding Monte Carlo simulation. The equiconcentration lines correspond to about  $2 \cdot 10^{20} \text{ cm}^{-3}$ ,  $2.3 \cdot 10^{19} \text{ cm}^{-3}$ , and  $2 \cdot 10^{18} \text{ cm}^{-3}$ .

as tabulated quantity allows very accurate interpolation in a small table.

### 3 Comparison of 2-D Simulation and Experiment

$140 \text{ keV}$  boron has been implanted into a  $\langle 100 \rangle$  wafer by a vertical mask edge with a dose of  $5 \cdot 10^{15} \text{ cm}^{-2}$ . The beam is  $7^\circ$  tilted such that the projection of the incidence direction to the wafer surface is parallel to the mask edge ( $\langle 010 \rangle$  direction). The sample has been annealed for 10 seconds at  $1000^\circ\text{C}$ . Equiconcentration lines have been determined by a delineation technique reported earlier [21].

The simulation has been performed with the program described in the previous sections. A point response has been computed and superposed to obtain the distribution near the edge of an impenetrable mask. It is known from simulations [22] and experiment [23] that the concentration close to the surface near a vertical mask edge is not identical to that near an impenetrable mask. This is because in a vertical mask edge ions are scattered out of the mask and enter the silicon region producing an additional concentration there. As these ions are slowed down in the mask they penetrate only to shallower depths in the silicon. For this reason the shallow part of the dopant distribution cannot be compared. Figure 2 shows both experiment and simulation. In the experiment the mask covers the right part of the surface whereas in the simulation it covers the left part. Notice that in both cases the equiconcentration lines run approximately  $45^\circ$  tilted from the maximum lateral to the maximum vertical penetration. Also, the distance between the two lower equiconcentration lines agrees very well except near to the surface.

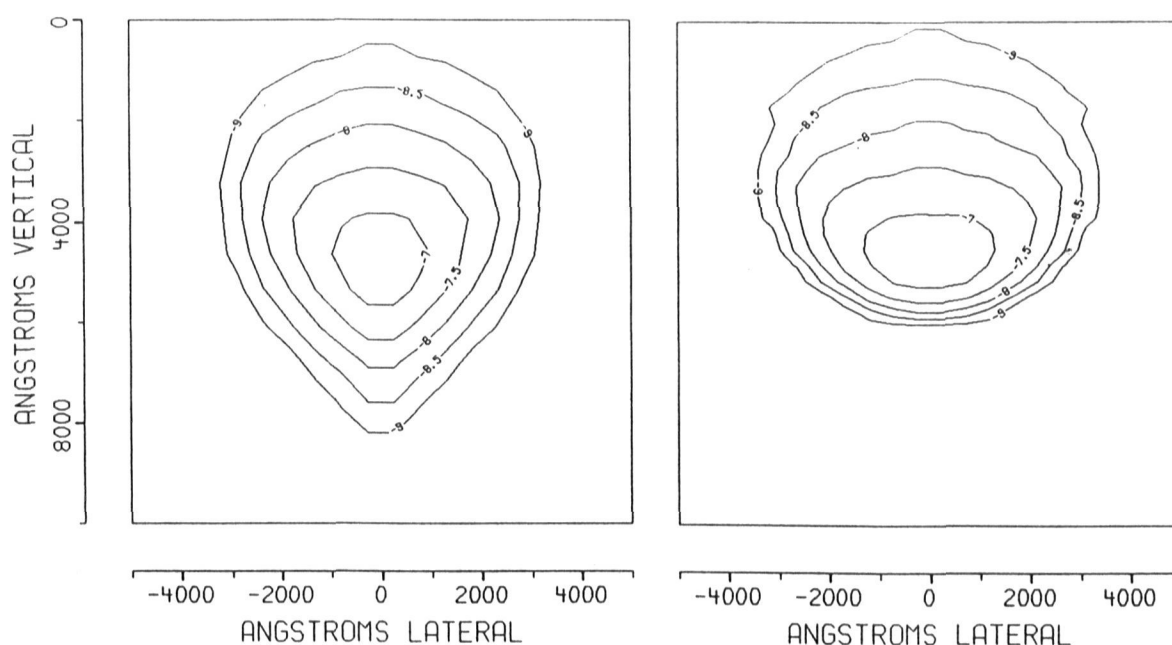


Figure 3: Point response in crystalline (left) and amorphous silicon (right). Same implantation conditions as in Figure 2. The ions enter the target at the center of the top surface. The contour lines represent the logarithm of the concentration (arbitrary units).

#### 4 Comparison of Dopant Distributions in Crystalline and Amorphous Silicon

The point responses in crystalline and amorphous silicon are shown in Figure 3. The beam is  $7^\circ$  tilted such that the lateral component of the incidence direction is parallel to the direction of view ( $\langle 010 \rangle$  direction). Therefore the crystalline point response appears symmetric. A very similar behaviour in the crystalline and amorphous case is seen at depths up to about the mean projected range. The channeling tail is closely centered around the  $\langle 100 \rangle$  axis. This indicates that axial channeling in the  $\langle 100 \rangle$  direction dominates over, e. g.,  $\langle 110 \rangle$  channeling.

It should be mentioned that channeling in other directions than  $\langle 100 \rangle$  exists. This can be seen in Figure 4 where one more equiconcentration line is shown. Although some jitter is obviously present, the same qualitative behaviour is also seen in other simulations. Especially at low implantation energies more pronounced tails along other directions than  $\langle 100 \rangle$  form. In Figure 4b the point response is observed from a direction which is rotated by  $45^\circ$  with respect to Figure 4a. Now  $\langle 011 \rangle$  is the direction of view. It can be seen that the point response is not rotational symmetric.

Figure 5 shows the 1-D profiles together with the lateral standard deviation and the lateral kurtosis as a function of depth. A similar behaviour of the lateral moments in crystalline and amorphous silicon is again observed up to the mean projected range. In the channeling tail a completely different behaviour is seen: The standard deviation has a second moderate peak, the kurtosis has a very high sharp peak. It seems difficult to find an analytical model for the depth dependent lateral moments as a function of implantation energy like in the case of amorphous silicon [24].

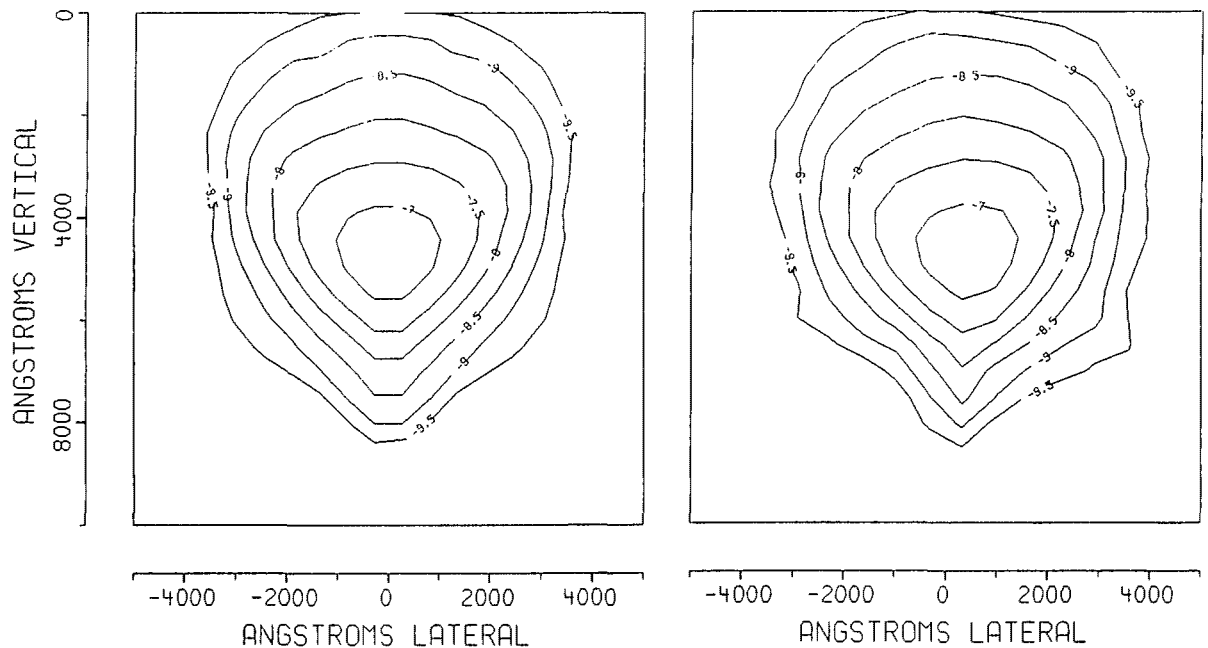


Figure 4: Point response in crystalline silicon showing other channeling than in  $\langle 100 \rangle$  direction. Same implantation conditions as in Figure 2. Left: direction of view  $\langle 010 \rangle$ . Right: direction of view  $\langle 011 \rangle$ . The contour lines represent the logarithm of the concentration (arbitrary units).

## 5 Summary and Conclusions

Boron implantations into crystalline silicon can be excellently simulated both in 1-D and 2-D. In this paper implantation energies of 140/150 keV have been investigated. Simulations and experiments at lower energies indicate that at least in 1-D very good agreement exists at energies as low as 5 keV. No investigations above 150 keV have been performed so far. Also, we have made no attempt until now to calculate implantation damage and its effect on the implantation profile. In the 1-D experiments leading to our electronic stopping power model, the implantation dose was low enough to preclude any damage effects. In the 2-D experiment some damage could have been present. However, the dose was still well below the amorphization limit.

It has been shown that in  $\langle 100 \rangle$  wafers  $\langle 100 \rangle$  channeling dominates. This could be different at very low implantation energies. Ions channeled along other directions appear at low concentrations. This might prohibit extrapolation of the doping distribution obtained by the Monte Carlo method to lower concentrations. It should be noted that the investigation of this regime poses a serious computation time problem as each extension of the concentration range by a factor of 10 requires an increase in particle number by a factor of 10 and thus an increase in computation time by a factor of 10. The simulation in Figure 4 took 4 CPU days on a 7.5 Mflops IBM Riscstation 6000 using 200000 particles (MARLOWE would take about the same time for the same number of particles). Nevertheless, it has been shown that useful 2-D Monte Carlo simulations of ion implantation in crystalline targets can be performed with today's computer power.

*Acknowledgement* — This work has been supported by the Fonds zur Förderung der wissenschaftlichen Forschung, project no. P7495-PHY.



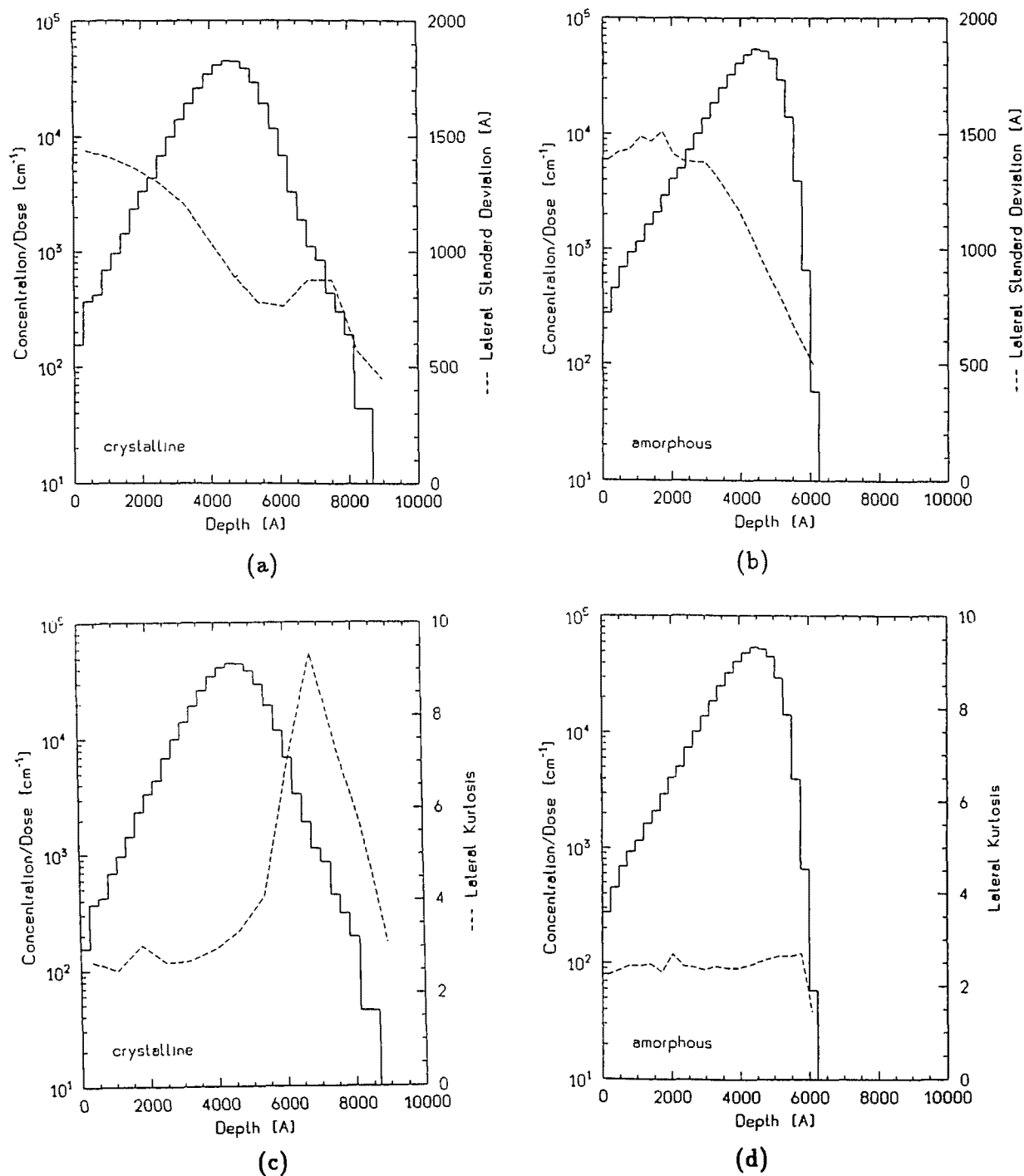


Figure 5: 1-D profile with depth dependent lateral standard deviation (a,b) and depth dependent lateral kurtosis (c,d). Crystalline target left (a,c), amorphous target right (b,d). Same implantation conditions as in Figure 2.

## References

- [1] A. Desalvo, R. Rosa: "Monte Carlo Calculations on Spatial Distribution of Implanted Ions in Silicon", *Rad. Eff.*, Vol. 31, pp.41-45, 1976.
- [2] A. M. Mazzone, G. Rocca: "Three-Dimensional Monte Carlo Simulations — Part 1: Implanted Profiles for Dopants in Submicron Devices", *IEEE Trans. Comp.-Aided Des.*, Vol. 3, No. 1, pp. 64-71, 1984.
- [3] M. Hane, M. Fukuma: "Ion Implantation Model Considering Crystal Structure Effects", *IEEE Trans. Electron Dev.*, Vol. 37, No. 9, pp. 1959-1963, 1990.
- [4] N. Azziz, K. W. Brannon, G. R. Srinivasan: "Impact Parameter Dependent Electronic Energy Losses", *Phys. Stat. Sol.*, Vol. B 142, pp. 35-47, 1987.
- [5] K. M. Klein, C. Park, A. F. Tasch: "Local Electron Concentration-Dependent Electronic Stopping Power Model for Monte Carlo Simulation of Low-Energy Ion Implantation in Silicon", *Appl. Phys. Lett.*, Vol. 57, No. 25, pp. 2701-2703, 1990.
- [6] G. Hobler, H. Pötzl, L. Palmethofer, R. Schork, J. Lorenz, C. Tian, S. Gara, G. Stinger: "An Empirical Model for the Electronic Stopping of Boron in Silicon", *Proc. NASECODE VII*, pp. 85-86, 1991.
- [7] M. Hou, M. T. Robinson: "Computer Studies of Low Energy Scattering in Crystalline and Amorphous Targets", *Nucl. Instr. Meth.*, Vol. 132, pp. 641-645, 1976.
- [8] B. J. Mulvaney, W. B. Richardson, T. L. Crandle: "PEPPER — A Process Simulator for VLSI", *IEEE Trans. Comp.-Aided Des.*, Vol. 8, No. 4, pp. 336-349, 1989.
- [9] M. T. Robinson: *MARLOWE Version 12, User's Guide*, Oak Ridge National Laboratory, Oak Ridge, Tennessee 37831.
- [10] G. Hobler, H. Pötzl, R. Schork, J. Lorenz, S. Gara, G. Stinger: "Channeling of Boron in Silicon: Experiments and Simulation", *Proc. ESSDERC 90*, pp. 217-220, 1990.
- [11] J. F. Ziegler, J. P. Biersack, U. Littmark: "The Stopping and Range of Ions in Solids", Pergamon Press, 1985.
- [12] C. Park, K. M. Klein, A. F. Tasch, J. F. Ziegler: "Critical Angles for Channeling of Boron Ions Implanted into Single-Crystal Silicon", *Proc. 2nd Int. Symp. Process Physics and Modeling in Semiconductor Technology*, The Electrochem. Soc., pp. 94-106, 1991.
- [13] F. H. Eisen: "Channeling of Medium-Mass Ions through Silicon", *Can. J. Phys.*, Vol. 46, pp. 561-572, 1968.
- [14] O. B. Firsov: "A Qualitative Interpretation of the Mean Electron Excitation Energy in Atomic Collisions", *Sov. Phys. JETP*, Vol. 36(9), No. 5, pp. 1076-1080, 1959.
- [15] O. S. Oen, M. T. Robinson: "Computer Studies of the Reflection of Light Ions from Solids", *Nucl. Instr. Meth.*, Vol. 132, pp. 647-653, 1976.
- [16] J. Lindhard, M. Scharff: "Energy Dissipation by Ions in the keV Region", *Phys. Rev.*, Vol. 124, No. 1, pp. 128-130, 1961.
- [17] M. Blackman: "The Specific Heat of Solids", In: *Handbuch der Physik*, Vol. 7/1 (Ed. S. Flügge), pp. 325-382, 1955.
- [18] S. Alliney, F. Malaguti, E. Verondini: "The Effect of Correlated Thermal Vibrations on Crystal Blocking Patterns", *Nucl. Instr. Meth.*, Vol. B 28, pp. 10-16, 1987.
- [19] J. P. Biersack, L. G. Haggmark: "A Monte Carlo Computer Program for the Transport of Energetic Ions in Amorphous Targets", *Nucl. Instr. Meth.*, Vol. 174, pp. 257-269, 1980.
- [20] G. Hobler, S. Selberherr: "Efficient Two-Dimensional Monte Carlo Simulation of Ion Implantation", *Proc. NASECODE V Conf.*, pp. 225-230, 1987.
- [21] L. Gong, A. Barthel, J. Lorenz, H. Ryssel: "Simulation of the Lateral Spread of Implanted Ions: Experiments", *Proc. ESSDERC-89*, pp. 198-201, 1989.
- [22] G. Hobler, S. Selberherr: "Monte Carlo Simulation of Ion Implantation into Two- and Three-Dimensional Structures", *IEEE Trans. Comp.-Aided Des.*, Vol. 8, No. 5, pp. 450-459, 1989.
- [23] L. Gong, J. Lorenz, H. Ryssel: "Direct Observation of the Mask Edge Effect in a Boron Implantation", *Proc. ESSDERC 90*, pp. 93-96, 1990.
- [24] G. Hobler, E. Langer, S. Selberherr: "Two-Dimensional Modeling of Ion Implantation with Spatial Moments", *Sol.-State Electron.*, Vol. 30, No. 4, pp. 445-455, 1987.